



# Effect of Turbulence Intensity on Low Reynolds Number Airfoil Aerodynamics

Ashish Kumar Gupta\*, P. A. Aswatha Narayana, G. Ramesh

Dept. of Aerospace Engg., Jain University  
 NH-209, Jakkasandra Post, Ramanagara Dist.-562112, KK, India  
 \*Corresponding author E-mail: Ashish.kumar@gmail.com

## Abstract

The flow transition over the airfoil at low Reynolds number influences its aerodynamic performance; hence this is being studied by many researchers in the recent times. One of the important factors affecting flow transition is the turbulence intensity of the oncoming flow that has not been well addressed. Here a systematic study on a few of Low Reynolds number airfoils is made through viscous- inviscid interaction code XFLR to understand the sensitivity of the inlet turbulence on the flow transition. The analyses with XFLR5 code were made at three Reynolds number and three different turbulent intensity values. The analysis brings out clearly the sensitivity of the flow to turbulence intensity. The reason for the drag increase and scatter in the experimental data has been investigated which is seen in case of E387 airfoil for Reynolds number below 100,000.

**Keywords:** Aerodynamic performance; Low Reynolds number; Turbulent Intensity; Transition; XFLR.

## 1. Introduction

Chord based Reynolds number ( $Re = \rho V C / \mu$ ) is one of the important flow parameter that affects the performance of airfoils. Unlike high Reynolds number flows, low Reynolds number flows are characterized by complex flow features such as viscous flow, laminar flow separation, vortical flows, laminar to turbulent transition. Such flows are often encountered for MAV flight where the Reynolds number is usually less than 300,000 owing to the low flight speed and small mean aerodynamic chord (Fig. 1). It is known that the airfoil performance degrades rapidly as the Reynolds number decreases below 300,000 (Fig. 2). The flow over the airfoil often separates due to the presence of adverse pressure gradient over the suction surface of airfoil aft of the maximum thickness location. The development of laminar separated flow has large influence on the aerodynamic performance of the airfoil. The separated shear layer undergoes transition to turbulence due to the presence of Kelvin Helmholtz instability. Transition to turbulence is influenced by the flow Reynolds number, angle of attack and presence of turbulence in the free steam. For  $Re < 30,000$ , the separated shear layer may not transition to turbulence in time to reattach on the airfoil surface [1]. For higher Reynolds number, the transition to turbulence will occur relatively early leading to flow reattachment on the airfoil surface resulting in the formation of Laminar Separation Bubble (LSB) (Fig. 3). The laminar separation bubbles are either short type or long type [1-3]. While the short type affects the pressure distribution only locally, the long type affects the pressure distribution significantly including the peak suction pressure and hence reduces the lift coefficient,  $C_l$  [3]

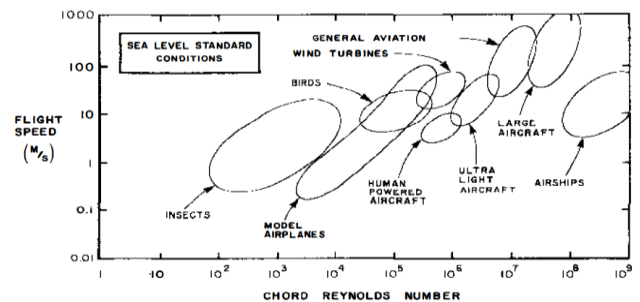


Fig. 1: Flight Reynolds number spectrum, Lissaman [4]

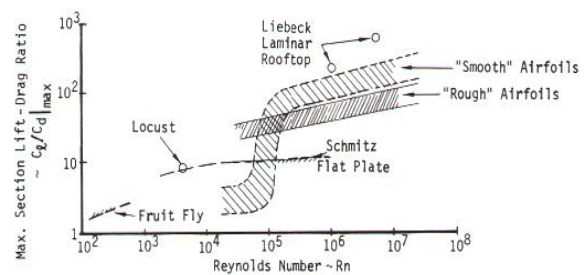


Fig. 2: Maximum Lift-to-Drag vs Reynolds number [5]

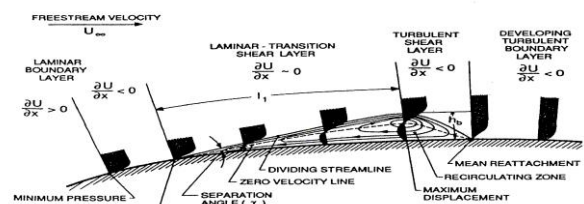


Fig. 3: Structure of laminar separation bubble [9]



Laminar to turbulent transition process involves wide range of scales, with energy and momentum transfer predominantly affected by non-linear (inertial) process. In addition, transition occurs through different mechanisms for different applications such as natural transition, bypass transition and separation induced transition [6, 8]. It is also believed that for the natural transition mode, a linear part of amplification covers a large percentage of the distance between first instability and transition, which is followed by the non-linear breakdown of instability to turbulent flow [7].

In an earlier study by Schmitz [10], it was observed that a thick cambered airfoil has a critical Reynolds number, where the airfoil performance changes drastically (Fig. 4a). Mueller [11] performed flow visualization and force measurements over NACA 663-018 airfoil at  $4 \times 10^4 < Re < 4 \times 10^5$ . The lift coefficient measurement at  $Re = 40,000$  and  $\alpha = 8^\circ$ , showed a drastic change in value. McArthur [9] points out that above a critical value of Reynolds number, lift to drag ratio (L/D) is much higher than the L/D ratio when the Reynolds number is reduced below the critical Re value (Fig. 4a). When the Reynolds number is below the critical Reynolds number value, the flow is dominated by viscous forces and boundary layer remains laminar over the entire airfoil.

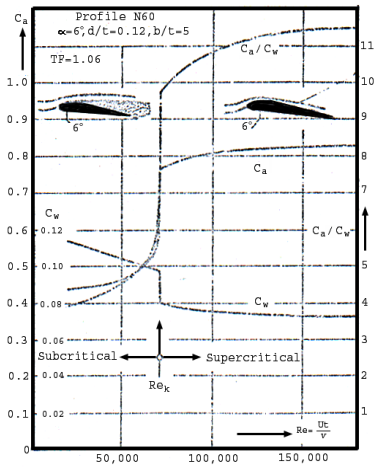


Fig. 4a: L/D ratio vs. Reynolds number- the critical Re [9]

It is known that transition to turbulent flow plays a critical role in determining the performance characteristics of an airfoil. As indicated earlier, the transition phenomenon is influenced by the flow Reynolds number, angle of attack and turbulence in the ambient atmosphere. In a series of extensive study over airfoil at low Reynolds number, lift and drag measurements were carried out on over 60 different airfoils [12]. The Reynolds number was varied from 60,000 to 300,000. It was observed that for  $Re > 100,000$ , the drag polars were qualitatively similar to drag polar at higher Reynolds number. But as Reynolds number decreased below above value, there was significant increase in drag at moderate  $C_L$  and the drag polar showed large scatter (Fig. 4b) in the measured data [9, 12] that were obtained from different wind tunnel measurements. The reason for drag increase and the scatter in the measured data are not clearly understood, although it is mentioned that varying amount of turbulence in different wind tunnels could be a reason. Selig [12] called this as bubble drag (drag due to LSB), while Grundy [13] calls drag due to long separation bubble, but not supported by any measurement.

In the present study, investigation has been made to understand the effect of free-stream turbulence in flow (or turbulent intensity) using Mark Drela program XFLR5 [14] over four airfoils namely E387, SD7037, MH45 and S1223. XFLR code is a viscous inviscid interaction code and has been used extensively for predicting low Reynolds number flow over airfoils. It incorporates  $e^N$  transition prediction method which is found to be successful in transition prediction for flow over airfoils.

## 2. Numerical Approach

In the direct mode, XFLR5 utilizes the viscous inviscid interaction method and computes inviscid outer flow over airfoil using linear vorticity stream function panel method, while the full inverse method, the code utilizes Lighthill and Van Ingen complex mapping method. The inviscid solution is used as input for solving the boundary layer and wake using two equation lagged dissipation integral boundary layer formulation and an envelope  $e^N$  transition prediction criteria. The XFLR calculations have been carried out for several airfoil sections mentioned above, for Reynolds number value of 60,000, 100,000 and 200,000, and angle of attack,  $\alpha$  varying from  $-6^\circ$  to  $16^\circ$ .

### 2.1. $e^N$ Envelope Method

The  $e^N$  method [7] is based on linear stability theory for a given laminar main flow with superimposed small disturbances upon it for an incompressible flow. For such flow, with certain assumptions, the Navier Stokes equations are reduced to Orr-Sommerfeld equation [7] if the disturbance field given by

$$\psi(y) = \varphi(y) \exp\{i(\alpha x - \omega t)\} \quad (1)$$

The above equation is a homogeneous linear equation in disturbance amplitude  $\varphi$ . Assuming,  $\alpha$  to be complex, the amplification factor  $n$  is then given by

$$n(x, \omega) = \ln(a/a_0) = \int_{x_0}^x -\alpha_i dx \quad (2)$$

Thus, for a given  $x$  location and different  $\omega$ , one can obtain the maximum amplification factor  $N$ , which is related to start and end

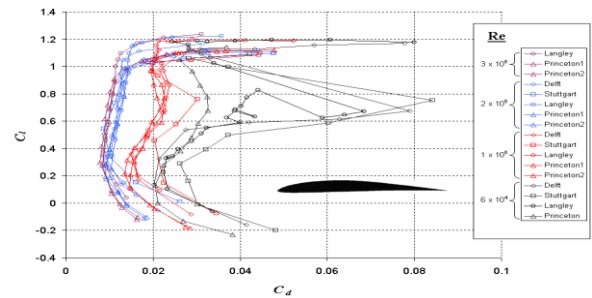


Fig. 4b: Drag polar for E387 [9]

of transition location ( $N_1, N_2$ ) based on experimental data from Schubauer and Skramstad [15]. The average of these two numbers is taken as  $N_{crit}$ . The  $N_{crit}$  will depend on, among other parameters, turbulent intensity of the flow. Dependence of  $N_{crit}$  on turbulent intensity is as below [7] –

$$N_1 = 2.13 - 6.18 \log(Tu) \quad (3a)$$

$$N_2 = 5.0 - 6.18 \log(Tu) \quad (3b)$$

It is seen that for  $Tu = 0.09\%$ ,  $N_{crit} = 10$ ,  $Tu = 0.4\%$ ,  $N_{crit} = 6$  and  $Tu = 1.2\%$ ,  $N_{crit} = 3$ . These values have been used while computing flow for different Reynolds number in the XFLR5 program.

## 3. Results and discussions

### 3.1 Comparison of Drag Polar and $C_L$ Versus $\alpha$

The analysis was carried out for three Reynolds number and for three turbulence level over four different airfoils. The drag polar

and  $C_l$  versus  $\alpha$  curve obtained for each airfoil have been shown in Fig. 5a & 5b, Fig. 6a & 6b, Fig.7a & 7b and Fig. 8a & 8b respectively, i.e. for airfoils E387, SD7037, MH45 and S1223.

turbulence intensity level of less than 0.1 % has been reported in the test section of the wind tunnel, which corresponds to  $N_{crit}$  value of 10. For instance, Fig 5a shows the comparison of experimental data ( $Tu = 0.1\%$ ) with XFLR results for  $Tu = 0.09\%$ ,  $0.4\%$  and  $1.2\%$ .

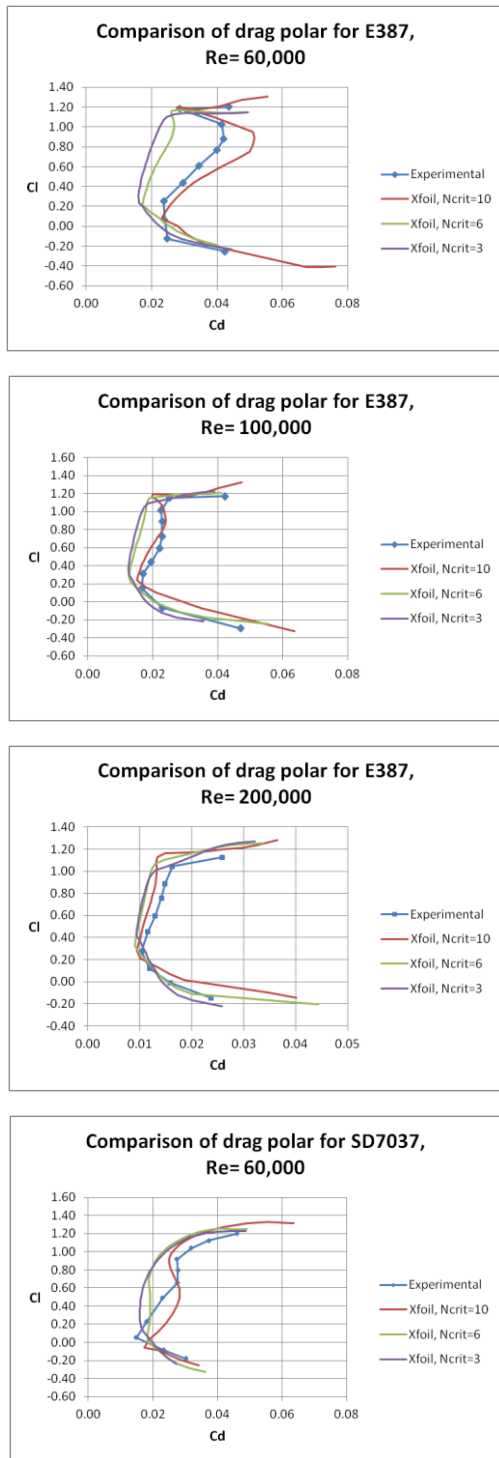


Fig. 5a: Drag polar curve for E387 different Re

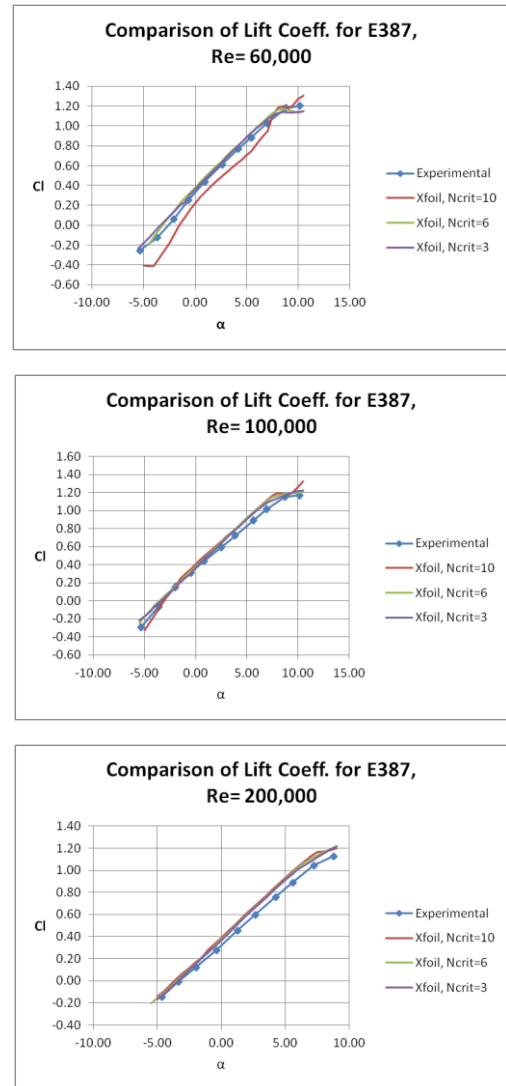


Fig. 5b:  $C_l$  versus  $\alpha$  curve for E387 different Re

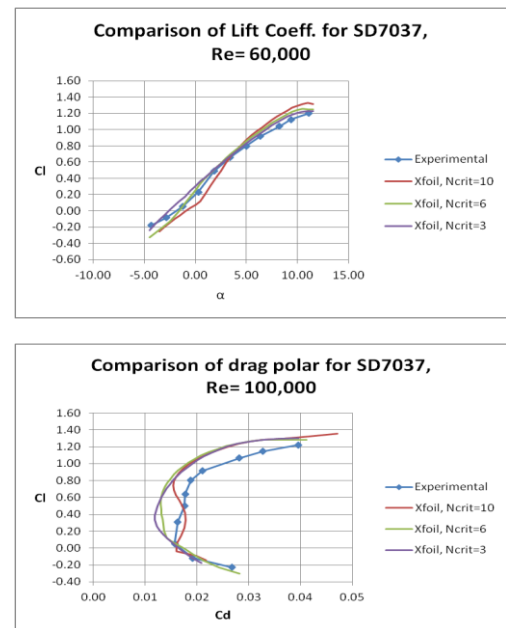


Fig. 9 shows the comparison of two experimental data from Selig [12] and McArthur [9] and its comparison with XFLR results corresponding to turbulence intensity value of 0.1% and 0.03% in experiment. It can be clearly seen from both experiment [9, 12] and XFLR results that as the turbulent intensity reduces, the drag increases for E387 and also there is large difference (or scatter) in the drag values for the two turbulent intensity values considered. At very low  $Tu$  value of 0.03 %, the comparison between experiment and XFLR result becomes worse. For S1223, there is no drag polar data for  $Re = 60,000$ . The experimental data have been obtained from wind tunnel measurements at UIUC [12, 17]. The

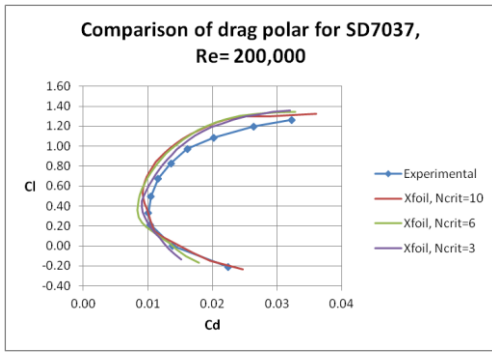


Fig. 6a: Drag polar curve for SD7037 different Re

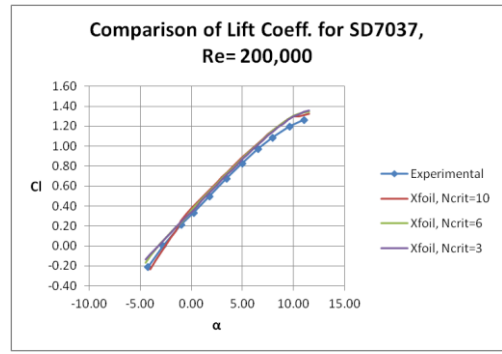


Fig. 6b:  $C_l$  versus  $\alpha$  curve for SD7037 different Re

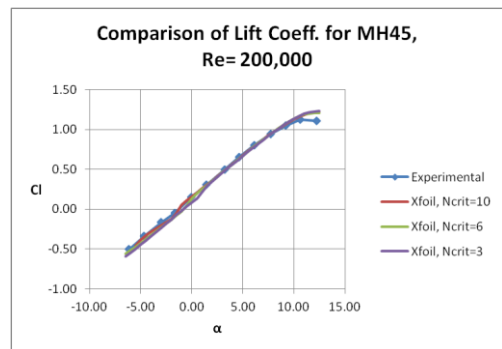
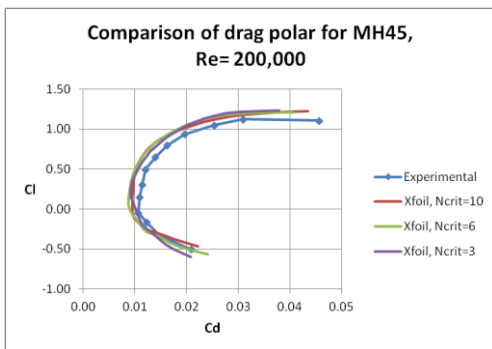
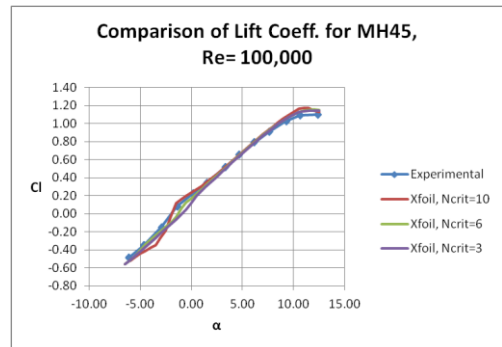
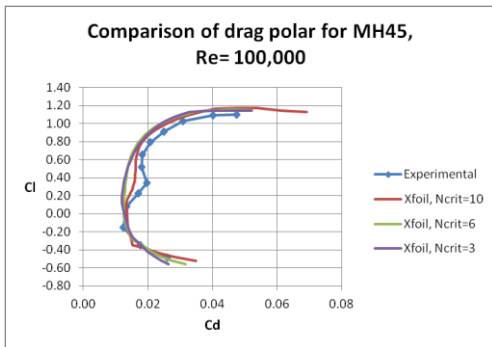
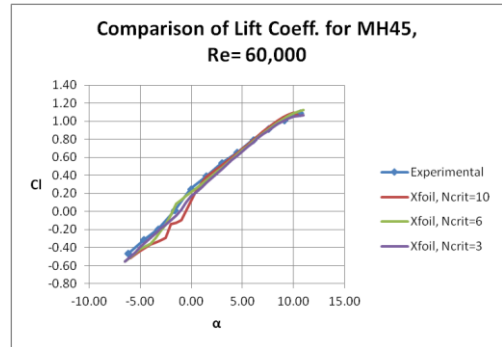
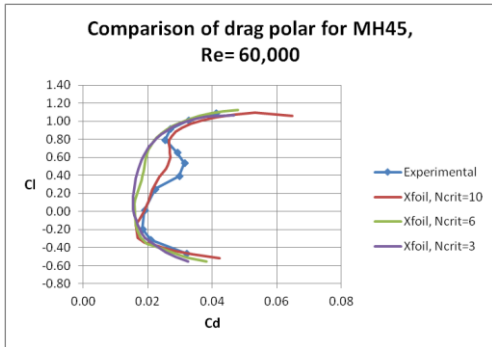
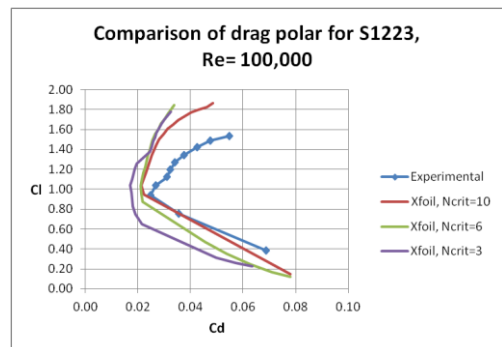
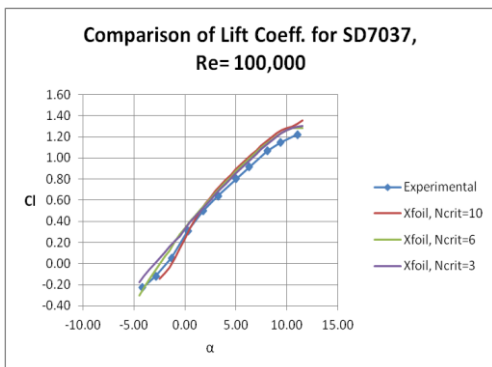


Fig. 7a: Drag polar curve for MH45 different Re

Fig. 7b:  $C_l$  versus  $\alpha$  curve for MH45 different Re



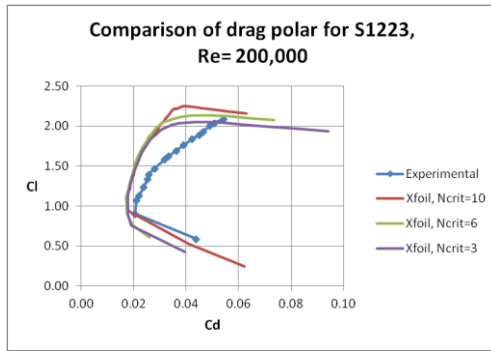


Fig. 8a: Drag polar curve for S1223 different Re

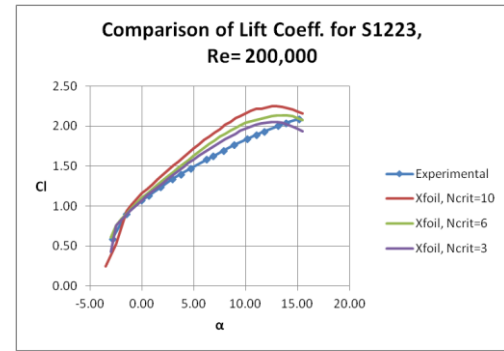


Fig. 8b:  $C_l$  versus  $\alpha$  curve for S1223 different Re

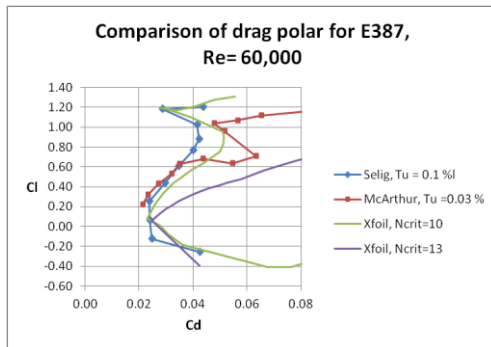
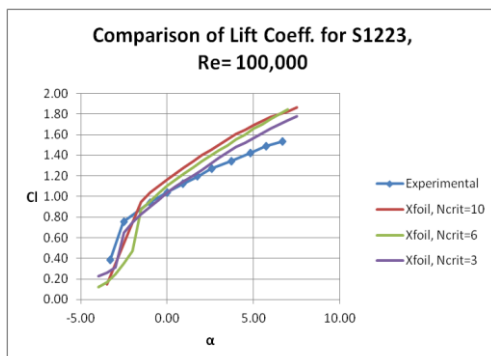


Fig. 9: Comparison of drag polar for  $Tu=0.03\%$  and  $Tu=0.1\%$  for XFLR5

The drag polar comparison has been fairly good for E387, SD7037 and MH45 airfoil sections while for S1223, even though the trends are captured, results do not match well. The  $C_l$  versus  $\alpha$  curve match with the experimental data is poor for  $Re = 60,000$ , while for  $Re = 100,000$  and  $200,000$  is fair. No specific reason could be assigned for poor match for S1223 airfoil. From the above plots, following important observations are made:

1. For  $Re = 60,000$ ,  $C_l$ - $\alpha$  curve using XFLR, do not compare well but it does show sensitivity to turbulence level for  $Tu=0.09\%$ , as it can be seen from above figures. For  $Re = 200,000$ , the  $C_l$ - $\alpha$  curves for XFLR results are coincident for different turbulence levels used in computation and hence is less sensitive to free stream turbulence.
2. For higher Reynolds number ( $Re = 200,000$ ), drag polar curve fall onto each other for different turbulent intensity values. Hence, for this Reynolds number, drag polar is relatively insensitive to free stream turbulence.
3. For relatively low Reynolds number ( $Re = 60,000$  and  $100,000$ ), drag polar curves are separated (or scattered) for different turbulent intensity levels used in computation. XFLR is able to capture the drag rise at moderate  $C_l$ , even though value may not match well. The scatter in drag polar for different turbulent intensity values is more as the Reynolds number reduces below  $100,000$  and for  $Tu$  less than  $0.1\%$ .



McArthur concludes that the drag rise observed for airfoils at Reynolds number below  $100,000$  (and it was observed especially for E387) was due to the laminar flow separation with no transition to turbulence and hence no reattachment of flow. Also, it was found that there is scatter in data obtained from different wind tunnels for E387 at  $Re = 60,000$ . While this is true, a stronger reason is that the flow is extremely sensitive to turbulence present in the free stream as the chord based Reynolds number approaches critical Reynolds number. Thus, at smaller turbulence levels ( $Tu < 0.1\%$ ), flow transition to turbulence does not occur and flow does not reattach giving rise to increased drag. Therefore, even small changes in the wind tunnel turbulence level or the model geometry roughness parameter, results in large scatter in the measurement data.

## 4. Conclusion

The numerical analysis using XFLR has been successfully used to study the effect of turbulence intensity on the aerodynamic performance of low Reynolds number airfoils. The large scatter in the drag polar data as seen in the results near the critical Reynolds number clearly brought out the effect of turbulence intensity on the performance of airfoils at these Reynolds number. This has also been verified with the experimental results from standard literature in the case of E387 airfoil. There is increase in drag at moderate lift coefficient at this Reynolds number and it is seen that it is inversely related to turbulent intensity in the flow. These results also highlight the fact that as Reynolds number approaches critical Reynolds number value, turbulent intensity plays an important role in the performance of airfoil characteristics. It turns out that  $e^N$  transition prediction approach is good for predicting airfoil drag at Reynolds number below  $100,000$ .

## References

- [1] Mueller T. J., "Aerodynamic Measurements at Low Reynolds Numbers for Fixed Wing Micro-Air Vehicles", Development and Operation of UAVs for Military and Civil Applications, Sept. 13-17, 1999, VKI, Belgium.
- [2] Gaster, M., "The Structure and Behavior of Laminar Separation Bubbles", R Aeronautical Research Council, R & M No. 3595, March 1967.
- [3] Leon Li, "Experimental Testing of Low Reynolds Number Airfoils for Unmanned Aerial Vehicles" MS Thesis, Graduate Department of Institute for Aerospace Studies, Univ. of Toronto, 2013.
- [4] Lissaman, P. B. S., "Low-Reynolds-Number Airfoils", Ann. Rev. Fluid Mech., 15: 223{239, 1983.
- [5] McMasters, J. H., and Henderson, M. L., "Low-speed single-element airfoil synthesis", Technical Soaring 4, 2 (1979), 1-21.
- [6] Pasquale, D. Di., and Rona, A., "A Selective Review of CFD Transition Models", 39<sup>th</sup> AIAA Fluid Dynamics Conference, 22-25 June 2009, San Antonio, Texas.
- [7] Van Ingen, J. L., "The  $e^N$  Method for Transition Prediction: Historical Review of Work at TU Delft" 38<sup>th</sup> Fluid dynamics Conference and Exhibit, 23-26 June 2008, Seattle, Washington.

- [8] Xuan Ge, "A Three-Equation Bypass Transition Model Based on Intermittency Function", MS Thesis, Iowa State University, Ames, Iowa, 2013.
- [9] McArthur, J., Aerodynamics of Wings at Low Reynolds Number", PhD Thesis, Faculty of the Graduate School, Univ. of Southern California 2007.
- [10] SCHMITZ, F. W. Aerodynamik des Flugmodells. C. J. E. Volckmann Nachf. E. Wette, Berlin-Charlottenburg, 1942.
- [11] MUELLER, T. J., AND BATILL, S. M. Experimental studies of separation on a two-dimensional airfoil at low Reynolds numbers. AIAA Journal 20, 4 (1982), 457–463.
- [12] Selig, M. S., Guglielmo, J. J., Broeren, A. P., Giguere, P., "Summary of Airfoil Data- Vol 1", SoarTech Publications, Virginia Beach, Virginia, 1995.
- [13] GRUNDY, T. M., KEEFE, G. P., AND LOWSON, M. V. Effects of acoustic disturbances on low re aerofoil flows. In Proc. Conf. on Fixed, Flapping and Rotary Wing Vehicles at Very Low Reynolds Numbers (Notre Dame, Ind., June, 2000), pp. 91–113.
- [14] Drela, Mark, "XFOIL: An Analysis and Design System for Low Reynolds Number Airfoils", Conference on Low Reynolds Number Airfoil Aerodynamics, Univ. of Notre Dame, June 1989.
- [15] Schubauer, G. B. and Skramstadt, H. K. "Laminar Boundary Layer Oscillations and Transition on a Flat Plate." Report NACA 909, 1948.
- [16] D. K. Walters, D. Cokljat, "A Three-Equation Eddy-Viscosity Model for Reynolds-Averaged Navier–Stokes Simulations of Transitional Flow" ASME, J. Fluids Engineering, 130, 121401/1-121401/14 (2008).
- [17] Selig, M. S., Lyon, C. A., Giguere, P., Ninnham C. P. and Guglielmo J., "Summary of Airfoil Data- Vol 2", SoarTech Publications, Virginia Beach, Virginia, 1996.
- [18] Gupta, A. K., Aswatha Narayana, P. A., Ramesh G., "Numerical Validation of Low Reynolds Number Airfoil for UAV", Communicated for Publication.
- [19] Gerakopoulos R., Boutilier M. S. and Yarusevych S. "Aerodynamic Characteristics of a NACA 0018 Airfoil at Low Reynolds Numbers", 40<sup>th</sup> Fluid Dynamics Conference and Exhibit,, 28 June- 1 July 2010, Chicago, Illinois.
- [20] Harsh P. Gupta, "Study of Axi-symmetric and Elliptic Jet Instability using Shooting method", Report, Dept. of Aerospace Engg., IIST, Thiruvanthpuram, 2017.
- [21] Ashish Kumar Gupta, P. A. Aswatha Narayana, "Numerical Validation of low Re Airfoil for UAV", Conference on Emerging Technologies & Applications of UAVs, IIAEM, Jain University, 22-23, March 2017.